AIP | Applied Physics Letters

Influence of hydrogen on chemical vapor deposition of tungsten on sputterdeposited TiN layers

S.L. Zhang, R. Palmans, J. Keinonen, C. S. Petersson, and K. Maex

Citation: Applied Physics Letters **67**, 2998 (1995); doi: 10.1063/1.114931
View online: http://dx.doi.org/10.1063/1.114931
View Table of Contents: http://scitation.aip.org/content/aip/journal/apl/67/20?ver=pdfcov
Published by the AIP Publishing

Influence of hydrogen on chemical vapor deposition of tungsten on sputter-deposited TiN layers

S.-L. Zhang[a)]
Royal Institute of Technology, Department of Electronics, Box Electrum 229, S-164 40 Kista, Sweden

R. Palmans
IMEC, Kapeldreef 75, 3001 Leuven, Belgium

J. Keinonen
University of Helsinki, Accelerator Laboratory, Hämeentie 100, SF-00550 Helsinki, Finland

C. S. Petersson
Royal Institute of Technology, Department of Electronics, Box Electrum 229, S-164 40 Kista, Sweden

K. Maex
IMEC, Kapeldreef 75, 3001 Leuven, Belgium

(Received 5 June 1995; accepted for publication 7 September 1995)

Tungsten (W) films are deposited on sputter-deposited TiN adhesion layers in a cold-wall chemical vapor deposition reactor, initiated with the deposition of a W nucleation layer by SiH_4 reduction of WF_6. H_2 is also introduced in the reactor for some depositions. The electrical resistivity and mechanical stress of the W films are found to be dependent on the underlying TiN layers as well as on the presence of H_2 during W nucleation layer deposition. A higher resistivity is obtained when the W is deposited on the TiN prepared at 250 °C than on the TiN prepared at 450 °C. For the W deposited on the low-temperature TiN, the resistivity is reduced by adding H_2 to the reactants during W nucleation layer deposition; while for the W deposited on the high-temperature TiN, the resistivity is almost insensitive to the H_2 addition. More oxygen and fluorine are found at the W–TiN interface for the W deposited on the low-temperature TiN than on the high-temperature TiN. Introduction of H_2 to the reactants during W nucleation layer deposition reduces the concentrations of interfacial fluorine and oxygen, in agreement with thermodynamic predictions. A lower film stress is obtained for the W deposited on the high-temperature TiN layers and/or with H_2 addition. The W films become less textured when H_2 is introduced to the reactants during W nucleation layer deposition. © *1995 American Institute of Physics.*

Chemical vapor deposition (CVD) of tungsten (W) using tungsten hexafluoride (WF_6) is attractive for contact or via filling in very-large-scale integration (VLSI) technology, owing to its low film resistivity of about 10 $\mu\Omega$ cm[1,2] and low deposition temperature typically at 250–450 °C.[1–6] W deposition from WF_6 is sensitive to the surface conditions.[3–9] This makes selective W deposition difficult if the surface of concern contains oxide and other contaminants even in trace amounts. Selective deposition of W into contact windows of various depths surrounded by dielectric materials further suffers from W creeping and lateral growth on top of the surface of the dielectric materials around shallow windows. Therefore, blanket deposition of W is preferred because contact windows of various depths can be filled up simultaneously. This concept relies on the deposition of an adhesion layer over the entire wafer surface prior to W deposition. Among many alternatives, titanium nitride (TiN) is a fairly good conductor with a resistivity of about 50 $\mu\Omega$ cm, and it is thermally stable which makes it a good diffusion barrier.[10] TiN adheres well on various surfaces and permits W deposition to occur on its own surface using a nucleation step involving silane (SiH_4) reduction of WF_6

Deposition of W on top of TiN has recently been studied by several groups.[11,12] Structural and mechanical properties have been of major concern. Our recent results[13] show that both the electrical resistivity and mechanical stress of W films are strongly dependent on the structure of the underlying TiN. In the present work, emphasis will mainly be placed on the impact of H_2 addition to the reactants during W nucleation layer deposition on the electrical and mechanical properties of the W films. It will be shown that the amounts of interfacial oxygen and fluorine are reduced and that the films become less textured by introducing a large amount of H_2 to the reactants during W nucleation layer deposition, leading to a decrease in both film resistivity and film stress.

Silicon substrates used in this study were 125 mm diam Si wafers with ⟨100⟩ orientation, covered with a 250 nm thick plasma enhanced CVD silicon dioxide film deposited at 400 °C. Ti and TiN layers were sequentially sputter deposited on the PECVD oxide, in the same sputter chamber without breaking the vacuum between the two deposition steps.[13] Two different TiN/Ti adhesion bilayer systems were prepared. The low-temperature-type bilayer (denoted as low-*T* TiN) consisted of 100 nm thick TiN on top of 20 nm thick Ti, both deposited at 250 °C (wafer susceptor temperature), whereas the high-temperature-type bilayer (denoted as high-*T* TiN) was composed of 80 nm TiN on top of 30 nm Ti, both deposited at 450 °C susceptor temperature. These thicknesses were all nominal values. The low-*T* TiN was found

---

[a)] Electronic mail: shili@ele.kth.se

TABLE I. Summary of measurement results of the 40 nm thick W nucleation layers and of about 200 nm thick bulk W layers on top of the nucleation layers.

TiN/Ti bilayer	Deposition of W nucleation layer	Total thickness of W (nm)	Resistivity of W ($\mu\Omega$ cm)	Stress of W (GPa)	Integrated intensity of W-(110), XRD
High-T	WF_6, SiH_4, H_2	39	19.6	1.52	317
Low-T	WF_6, SiH_4, H_2	41	22.0	3.83	2307
High-T	WF_6, SiH_4	41	19.3	1.55	419
Low-T	WF_6, SiH_4	39	23.4	4.17	2654
High-T	WF_6, SiH_4, H_2	244	12.7	1.13	1126
Low-T	WF_6, SiH_4, H_2	242	13.1	1.62	10007
High-T	WF_6, SiH_4	253	12.7	1.14	1056
Low-T	WF_6, SiH_4	241	13.4	1.72	14725

slightly (about 5 at. %) Ti deficient.[13] W deposition was performed in a cold-wall CVD reactor at 475 °C wafer susceptor temperature, which amounts to about 434–438 °C wafer temperature.[13] The nucleation step was performed at a chamber pressure of 4.5 Torr with SiH_4 reduction of WF_6. H_2 was also introduced in the reactor during the nucleation step for some depositions. The bulk W deposition was always performed at 80 Torr with H_2 reduction of WF_6. After W deposition, no heat treatment was performed.

Table I summarizes the electrical and mechanical measurement results for W films of two different thicknesses, i.e., about 40 nm thick nucleation layers and ~200 nm thick bulk W on top of the 40 nm nucleation layers. Clearly, the resistivity and stress of the W films are strongly influenced by the underlying TiN/Ti bilayers as well as by H_2 addition to the reactants during the deposition of W nucleation layers. As the resistivity values given are averaged ones calculated over the entire thickness of the W films, the higher resistivity of the W films deposited on the low-T TiN is thus attributed to the higher concentrations of interfacial oxygen (O) and fluorine (F) piling up at the W–TiN interface. The depth profiles of O and F, obtained by secondary ion mass spectrometry (SIMS), are shown in Fig. 1 for the W films of about 240 nm thickness on the TiN/Ti bilayers. The thicker W films were chosen so as to also reveal the O and F concentrations in the W bulk. It is clear that the amount of interfacial F is proportional to the amount of interfacial O, and that the concentrations of interfacial O and F at the W–TiN interface are higher for the W deposited on the low-T TiN than on the high-T TiN. As expected, the O and F concentrations in the W bulk are independent of the type of adhesion bilayer or of the W nucleation layer, because the same H_2 reduction of WF_6 process was used for deposition of all bulk W films.

Figure 2 shows the quantitative F concentration in atomic percentages versus depth (counting from the W surface) for the W nucleation layers of about 40 nm thickness, determined by nuclear resonance broadening (NRB).[14] The F concentrations are higher for the W deposited on the low-T TiN than on the high-T TiN, in agreement with the SIMS results. For the W films deposited on the low-T TiN, the F concentration is higher for the W deposition without H_2 addition to the reactants. The introduction of H_2 to the reactants does not affect the amount of interfacial F for the W deposited on the high-T TiN. Furthermore, the F peaks are all extending into the underlying TiN layer, and the degree of this extension strongly depends on the type of TiN. Fluorine penetrates through the entire low-T TiN layer of 100 nm thickness and the concentration of F in TiN is somewhat reduced by H_2 addition to the reactants. In contrast, it does not penetrate the high-T TiN layer of 80 nm thickness, and the concentration of F in this type of TiN is substantially reduced and insensitive to H_2 addition. In all cases, the F

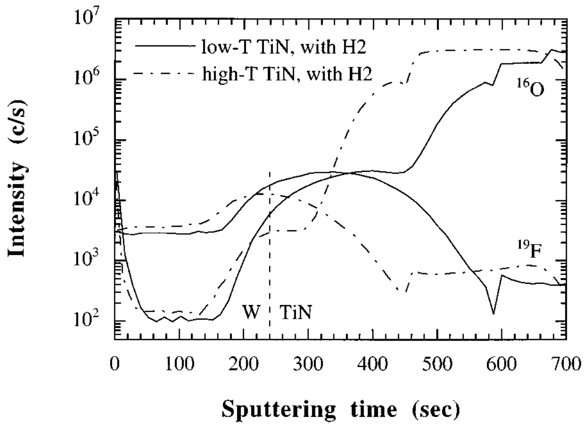

FIG. 1. SIMS results showing the O and F depth distributions in the W/TiN/Ti/SiO_2 structure for the W films of about 240 nm thickness for two different wafers. The broken vertical line indicates the approximate position of the W–TiN interface.

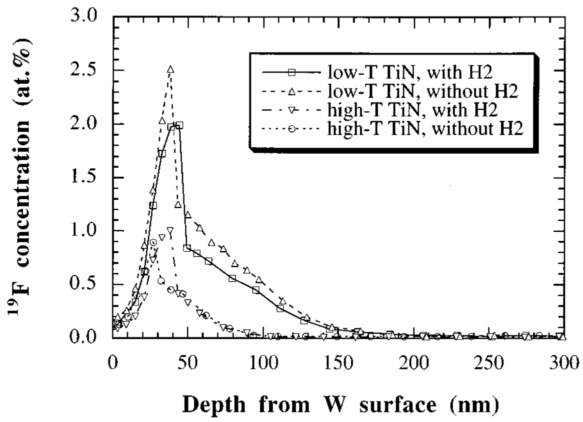

FIG. 2. NRB results of the F depth distributions, in atomic percentages, showing F piling up at the W–TiN interface and tailing considerably into the TiN layers for the W nucleation layers of 40 nm thickness.

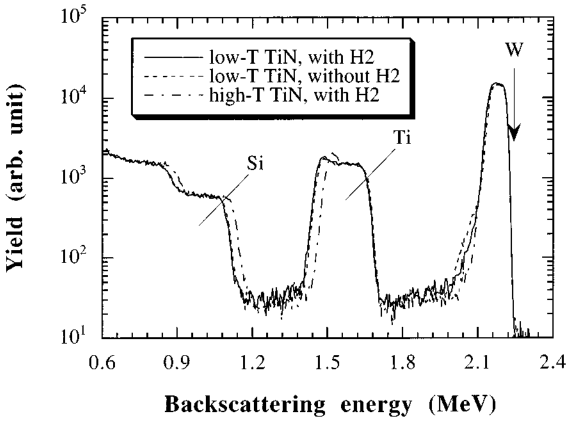

FIG. 3. RBS spectra for the W nucleation layers of 40 nm thickness depicting a small difference in the low-energy edge of the W peaks among the three wafers presented.

concentration decays rapidly from the peak values of 1.0–2.5 at. % at the W–TiN interface to about 0.1 at. % at the W surface (depth=0 nm) only about 40 nm apart. Presumably, most of the O impurities are also found in the similar depth range.

Tailing of F into the TiN layer is closely associated with the W penetration into the underlying TiN. The Rutherford backscattering spectrometry (RBS) results of Fig. 3 depict that the degree of extension of the low-energy edge of the W peaks towards lower energies follows the same trend as the degree of F tailing shown in Fig. 2. Since both the W surface and the W–TiN interface for the W nucleation layer deposited on the low-*T* TiN are smoother than those of the W nucleation layer deposited on the high-*T* TiN,[13] the W penetration into the underlying TiN is concluded to be the main cause for the extension of the low-energy edge of the W peaks observed in Fig. 3. Thus, depositing W on the high-*T* TiN or adding H_2 to the reactants during W deposition leads to reduced W penetration. It should, however, be noted that the depth of W extending into the underlying TiN is much shallower than the depth of F tailing into the same TiN. This is interpreted as a consequence of the much more rapid F penetration along the grain boundaries of TiN, as compared to W into TiN.

The interfacial O found at the W–TiN interface originates from native oxide on the TiN surface formed before W deposition.[13] Fluorine atoms pile up at the same interface because of the presence of O there. Large amounts of F atoms are incorporated at the W–TiN interface also due to the formation of nonvolatile TiF_3, a product of the chemical interaction between WF_6 and TiN under the deposition conditions used. Thermodynamic calculations predict that when a TiO_2 surface is exposed to the WF_6–SiH_4 mixture with a SiH_4-to-WF_6 ratio of about 0.5 and without H_2 addition, the main solid products will be WO_2, TiF_3, and W. H_2 addition to the same WF_6–SiH_4 mixture reduces the amount of solid oxide phase(s) by enhancing the formation of gaseous H_2O. The formation of TiF_3 will also be considerably reduced by H_2 as a result of increased amount of gaseous phase HF. On the other hand, when a TiN surface is exposed to the same WF_6–SiH_4 mixture, the impact of H_2 is almost negligible and the main solid products will always be TiF_3 and W. All these seem to be supported by the results of Figs. 1 and 2. Apparently, more oxidation takes place on the TiN surface of the low-*T* TiN, because this TiN has substantially more grain boundaries per unit surface area as compared to the high-*T* TiN.[13] The grains of the low-*T* TiN extend right through the whole TiN layer down to the underlying Ti layer. If sufficient F reaches the Ti underlayer, delamination can occur due to the interaction of F with Ti. The nonstoichiometric TiN layer also seems to promote the interaction between WF_6 and TiN. Therefore, to reduce the impurity level at the W–TiN interface, a stoichiometric TiN layer is preferred and a large amount of H_2 should be introduced to the WF_6–SiH_4 gas mixture during the deposition of W nucleation layers. The slight W penetration into the underlying TiN is ascribed to the inhomogeneous interaction between WF_6 and the partially oxidized TiN surface. The latter is formed because of nonuniform surface oxidation of TiN in air at room temperature.

The W films are all under tensile stress, and the amplitude of the stress is not only strongly influenced by the type of adhesion TiN/Ti bilayers,[13] but also affected by H_2 addition to the reactants during W nucleation layer deposition (see Table I). According to x-ray diffraction (XRD) analysis, the W films deposited are all preferentially oriented to the W ⟨110⟩, and the strong impact of the underlying TiN on the film texture of W has been reported elsewhere.[13] The integrated intensities of the W-(110) peak given in Table I are normalized values. The W films are less textured for the W deposited with H_2 addition to the reactants during the deposition of W nucleation layers. Thus, the difference in stress is attributed to the difference in the texture of the W films and possibly to the interfacial impurities as well.

The authors wish to thank J. Cardenas for SIMS and N. Lundberg for RBS. This work was financially supported by the Swedish Board for Technical Development (Nutek) and by the Flemish Institute for the Advancement of Scientific-Technological Research in Industry (IWT).

[1] M. L. Green and R. A. Levy, J. Electrochem. Soc. **132**, 1243 (1985).
[2] R. Palmans and K. Maex, *Advanced Metallization for ULSI Applications 1992*, edited by T. S. Cale and F. S. Pintchovski (Materials Research Society, Pittsburgh, PA, 1993), p. 57.
[3] E. K. Broadbent and C. L. Ramiller, J. Electrochem. Soc. **131**, 1427 (1984).
[4] K. Y. Tsao and H. H. Busta, J. Electrochem. Soc. **131**, 2702 (1984).
[5] H. H. Busta and C. H. Tang, J. Electrochem. Soc. **133**, 1195 (1986).
[6] E. K. Broadbent, J. Vac. Sci. Technol. B **5**, 1661 (1987).
[7] M. L. Green, Y. S. Ali, T. Boone, B. A. Davidson, L. C. Feldman, and S. Nakahara, J. Electrochem. Soc. **134**, 2285 (1987).
[8] M. Wong, N. Kobayashi, R. Browning, D. Paine, and K. C. Saraswat, J. Electrochem. Soc. **134**, 2339 (1987).
[9] J.-T. Wang, C.-B. Cao, H. Wang, and S.-L. Zhang, J. Electrochem. Soc. **141**, 2192 (1994).
[10] H. Norström, S. Nygren, P. Wiklund, M. Östling, R. Buchta, and C. S. Petersson, Vacuum **35**, 547 (1985).
[11] S. Sivaram, M. L. A. Dass, C. S. Wei, B. Tracy, and R. Shukla, J. Vac. Sci. Technol. A **11**, 87 (1993).
[12] J. Schmitz, S. Kang, R. Wolters, and K. van den Aker, J. Electrochem. Soc. **141**, 843 (1994).
[13] S.-L. Zhang, R. Palmans, S. Petersson, and K. Maex (unpublished).
[14] H. J. Whitlow, Th. Ericsson, M. Östling, C. S. Petersson, J. Keinonen, and A. Anttila, Appl. Phys. Lett. **50**, 1497 (1987).